Available online at www.sciencedirect.com

ScienceDirect

Transportation Research Procedia 72 (2023) 997–1004

Transportation Research Procedia

www.elsevier.com/locate/procedia

Transport Research Arena (TRA) Conference

Flapping-foil thrusters augmenting ship propulsion in waves

K. Belibassakis[a,*], J. Vermeiden[b], N. Townsend[c], N. Bulten[d], A. Öster[e]

[a] *School of Naval Architecture & Marine Engineering, National Technical University of Athens, Greece.*
[b] *Huygens Engineers, the Netherlands.*
[c] *Faculty of Engineering and Physical Sciences, University of Southampton, UK.*
[d] *Wartsila R&D and Engineering, Marine Power Solutions, the Netherlands.*
[e] *Wartsila R&D and Engineering, Marine Power Solutions, Vaasa, Finland.*

Abstract

Flapping-foil thrusters arranged at the bow of the ship are examined for extraction of energy from wave motions by direct conversion to thrust, offering also dynamic stability and reduction of added wave resistance. In the framework of H2020 Seatech project the above innovation, combined with standard propulsion system based on optimally controlled Dual Fuel engine, is examined, aiming at an increase in fuel efficiency and radical emission reductions. Results from the development and laboratory testing of tank-scale models of the considered biomimetic system and its performance in waves are presented, as obtained by active and passive control. The experiments provide useful data for the calculation of the combined performance with the propulsion system, and establish design requirements and methodologies to extend predictions to large models that will be tested at sea and to full scale.

Keywords: augmenting ship propulsion in waves; biomimetic thruster; towing tank experiments

1. Introduction

Ships operating in waves experience wave induced motions, additional resistance, powering requirements and greatly increased fuel consumption compared to calm water conditions, that typically could be of the order of 25% on average in a realistic utilisation profile. This negatively impacts the vessel's emission profile and operational cost. Extensive research concerning flapping-foil thrusters, including numerical modelling and experimental verification, has shown that the above systems, operating under conditions of optimal wake formation, can achieve high levels of propulsive efficiency; see, e.g., Triantafyllou et al (2000). The flapping-foil motion involves two oscillatory motions

* Corresponding author. Tel.: +30-2107721138;
E-mail address: kbel@fluid.mech.ntua.gr

10.1016/j.trpro.2023.11.528

heave and pitch with appropriate phase difference and a forward speed motion with the most energy demanding motion being the heave oscillation, Wu et al (2020).

In real sea conditions, the ship undergoes moderate or higher-amplitude oscillatory motions, due to waves. In this case, the ship motions could be exploited for providing the foil heaving motion free of cost, especially if the foil is located at the bow, as studied by various authors; see, e.g., Belibassakis & Politis (2013), Bøckmann & Steen (2016), Bowker et al (2020), Rozhdestvensky & Htet (2021). Moreover, in Filippas et al (2021) a nonlinear BEM approach is developed and verified against CFD models and used to study the active control of oscillating hydrofoils operating as unsteady thrusters augmenting ship propulsion in waves. One innovation within the Seatech H2020 project (https://seatech2020.eu/) is that of a dynamic wing arranged at the bow ship, as shown in Fig. 1, operating as an unsteady flapping thruster, which converts wave induced ship motions (wave energy) into a net additional thrust force (augmented propulsion) and contributes to the reduction of added wave resistance. The above system is examined, in combination with standard propulsion system based on optimally controlled Dual Fuel engine, aiming at an increase in fuel efficiency and radical emission reductions of NOx, SOx, CO_2 and particulate matter.

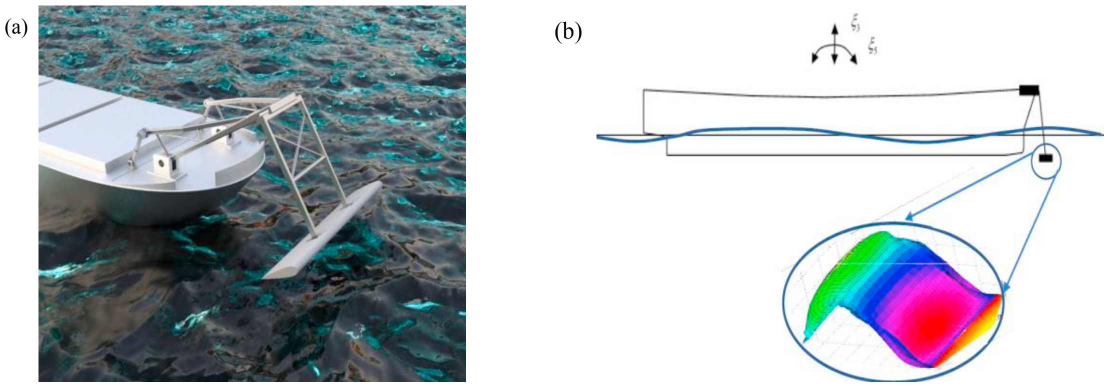

Fig.1. (a) Flapping thruster arranged at the bow of the ship and equipment for elevating/lowering the system in the water. (b) Ship hull in heaving and pitching motion in waves equipped with a flapping thruster below the keel, in front of the bow. The vertical foil motion is provided, free of cost, from ship responses, and the self-pitching motion is set by active or passive control. The shed vorticity in the flapping thruster wake is shown by using colour.

In this work, the development and laboratory testing of two tank-scale models of the biomimetic thruster with selected ship hull models are presented: one with active control tested at the National Technical University of Athens (NTUA) and another with passive control tested at the Southampton University (UoS) towing tanks, respectively, and the results obtained are shown and discussed. The experiments provide useful data in order to validate the numerical prediction tools and further calibrate the thrust-power coefficient charts that will be used for the calculation of the combined performance with the standard propulsion system of the ships and establish design requirements and methodologies to extend predictions to large model scale that will be tested at sea. The results will support the design of full-size wing including strength, fatigue and service-life considerations, as well as actuation and mechanical wing-retractability system for calm and heavy weather conditions, respectively.

2. Methodology and main contributions

The two ship hull models correspond to a Ferry ship (slender hull) and a small-size Bulk Carrier (full hull form). The models have been studied and tested with actively and passively controlled dynamic wings at the bow in the towing tanks of NTUA and UoS, respectively. The hull parameters are listed in Table 1 and the corresponding body plans are shown in Fig. 2. Photos of the two tank models during the tests in the tanks are shown in Fig.3, respectively. The hydrostatic particulars and main data of the two model hulls are listed in Table 1.

NTUA conducted model scale towing tank experiments to assess the hydrodynamic performance of the SeaTech dynamic wing for a car ferry model of length *L*=3.3m; see Fig.2(a). Seakeeping tests in regular and irregular head seas, without and with the operation of the actively controlled dynamic wing are performed.

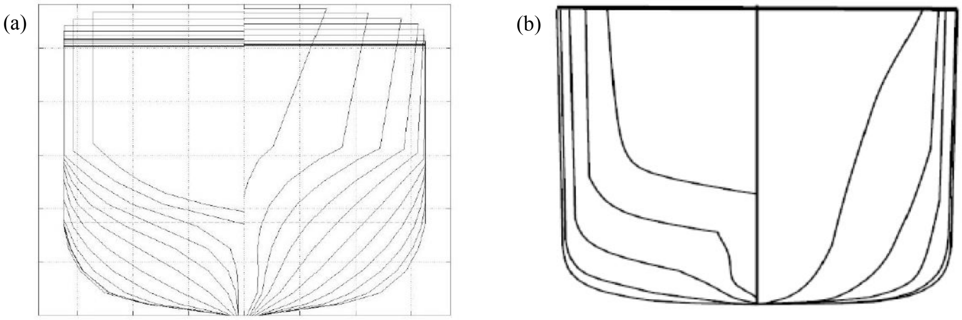

Fig. 2. Body plan of (a) Ferry Ship model and (b) small-size Bulk Carrier model.

Table 1: Hydrostatic particulars and data of the UoS and NTUA Seatech models

Vessel Type	Ferry Ship (twin screw)	Small Bulk Carrier (Single screw)
Scale Ratio	1:34	1:50
Overall Length (L_{oa})	3.3m	2.0m
Length between perpendiculars (L_{pp})	3.3m	2.0m
Waterline Length (L_{wl})	3.3m	2.0m
Breath (B) (Beam max extents on WL)	0.43m	0.33m
Draught (T) (Draft Amidships)	0.135m	0.120
Freeboard	0.265m	0.173m
Block Coefficient (C_b)	0.471	0.650
Prismatic Coefficient (C_p)	0.563	0.691
Length to Beam Ratio (L/B)	7.67	6.06
Beam to Draught Ratio (B/T)	3.18	2.75
Displacement (calc from vol, rho=1000 and 1025kg/m^3)	87.2kg	51.5kg
VCG	0.10m	0.14m
Wetted Surface Area	1.405m2	0.836m2
Max Sect. area coefficient (C_m)	0.836	0.943
Waterplane area coefficient (C_{wp})	0.730	0.826

UoS developed and manufactured a representative free running ship hull (L=2m) corresponding to a small-size Bulk Carrier shown in Fig.2(b), with an interchangeable foil assembly. A series of tests in calm water and regular waves with and without a spring loaded passively controlled foil were conducted at UoS and used to establish the performance in regular and irregular waves by directly measuring the delivered power and vessel motions using state-of-the-art video motion capture system (Qualysis).

2.1 Engineering for the NTUA towing tank model

The detailed functional specifications and working principles for the small-scale NTUA flapping thruster model using a foil with NACA0012 sections have been studied, and the final design together with the developed Control System (CS) are shown in Fig.4. The control system is based on the reading of the angle of attack of the flow in front of the dynamic wing, using the angle of attack meter (vane) which is also shown in Fig.4. The system accepts the following input data: O=offset, G=gain, D=delay, and performs the following functions (see Fig.4):

a) The dynamic angle of attack is measured using potentiometer providing input $\alpha(t)$ to the CS.
b) The foil angle is also measured by using a potentiometer providing input $\theta(t)$ to the CS.
c) The CS instructs the motor to rotate in order to force the linear actuator and rotate the crankshaft oscillating the vertical rods and transmit the angular motion $\theta(t)$ to the foil which is set equal to: $\theta(t) = Ga(t-D) + O$.

The input signal from the angle of attack meter is low pass filtered as follows: (i) 0-6 Hz, Gain=1/ripple 2.75dB, and (ii) 18-104 Hz, Gain 0/Actual attenuation -43dB. The sampling rate is set to 208Hz.

Fig. 3. Ship model testing of (a) NTUA Ferry model, and (b) UoS Bulk Carrier models.

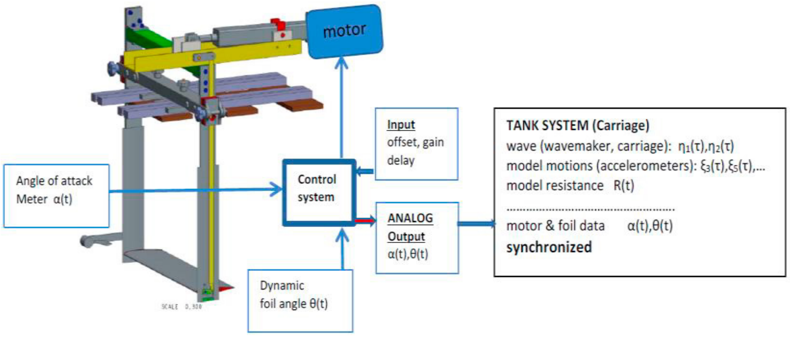

Fig. 4. The control system for the NTUA tank-scale model. The CS is a custom design board based on an ST microelectronics STM32F429 ARM mcu, running at 168 MHz.

Fig. 5. Functionality testing of the dynamic wing and control system in NTUA towing tank.

The output is synchronized with the towing tank acquisition system, providing simultaneous records of the following data for given tank carriage speed (model speed):

a) wave elevation from wavemaker and near the tank carriage (near the vessel): η_1(t), η_2(t)
b) ship model motions (heave and pitch of the hull from tank accelerometers): ξ_3(t), ξ_5(t)
c) the model resistance in the presence of waves with the dynamic foil in operation: R(t)
d) the angle of attack α(t) and the foil angle θ(t)

The firmware is based on FreeRTOS real time operating system. The control board provides the functions:

- Analog input for the AoA sensor. Oversampled at 2048 Hz and low pass filtered at 6Hz.
- Digital serial output to Animatics/Moog brushless servo motor (actuator).
- 5x12 / 3x12 bits spare analog outputs for monitoring and inputs for interfacing auxiliary sensors

- 3D gyroscope and 3D accelerometer and 3D magnetometer and pressure sensor.
- GNSS and WiFi / Bluetooth, GPRS /2G / 3G, and CAN Bus interface and uSD card for data acquisition.

The firmware implements various control and RTK kinematics algorithms assisting global positioning and real time spectral analysis, such as: (i) Quaternion estimation and Euler angles, (ii) Linear acceleration and speed.

The functionality testing of the dynamic wing and control system together with the motor in the water at NTUA towing tank is shown in Fig. 5. The system is used in experimental tests for the measurement of the flow angle of attack on the foil and the positioning of the dynamic wing and continuous recording of data, as well as of the obtained ship responses.

2.2 Engineering for the UoS towing tank model

The UoS free-running model Bulk Carrier, representative of a short sea cargo vessel, was designed and manufactured based on a collected database of 478 cargo carrying ships up to 10,000dwt. The model provides a generic representation of short sea vessels of around 100m in length. The model free-running bulk-carrier was tested with a passive sprung loaded, neutrally buoyant NACA0012 bow foil. The foil was mounted at 10% of the model length forward of the bow, which ensured that the foil operated in the free undisturbed flow stream. The spring-loaded foil was free to pitch up to +/- 45 degrees, pivoting at 10% of the chord length (from the leading edge), and measured using an encoder linked to a parallel pitching rod. Torque springs, located at the top and bottom of the pitching rod, were used to ensure a symmetric spring load. A numerical model based on previous work (Bowker & Townsend 2021) was used to derive the spring constant and foil size (AR=7). The entire bow foil component was secured to a protruding aluminium structure at the bow via a tri-axial load cell, as shown in Fig. 6. The propeller selection was based on the Gawn propeller series and a target thrust of 2.5N based on a calm water resistance estimate at the design speed 0.8m/s (F=0.18) with 50% sea margin. The developed drivetrain is shown in Fig.7.

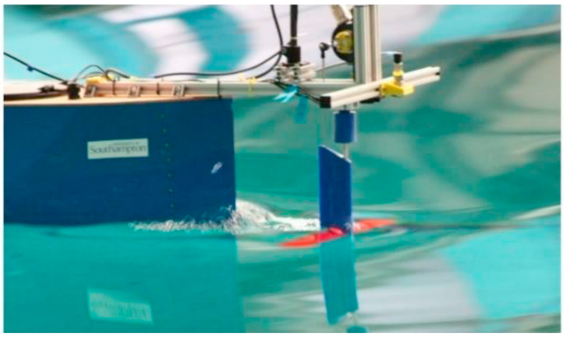

Fig. 6 UoS tank-scale model used for tests.

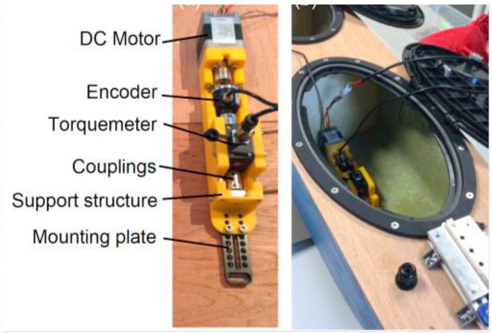

Fig.7 Instrumented model with propeller drivetrain and foil rig.

2.3 Test cases

The design Froude number concerning the NTUA model is F=0.25 (V_s=1.42m/s) and the cases for the tank scale model tests are listed in Table 2. In this case only head waves are considered and details are listed in Table 2. The design Froude number concerning the UoS model is F=0.17 (V_s=0.8m/s) and the cases for the tank scale model tests are listed in Table 3. The model is tested in regular head waves, selected to capture the peak frequencies of the equivalent full scale (Ls = 100m) ITTC sea state of Hs = 2m and T = 7s. The experimental test matrix is provided in Table 3.

3. Experimental results

The calm water resistance of the NTUA model at the two drafts without and with the flapping thruster, as shown in Fig.8, is measured and indicative results are presented in Fig. 10(a), where the total resistance coefficient

$C_T = R_{tot} / \left(0.5\rho S V^2\right)$ is plotted against the Froude number $F = V / \sqrt{g L_{BP}}$. Tank tests of the hull model in waves are then performed for the conditions listed in Table 2, as shown in Fig.9.

Table 2. Test cases of the NTUA tank-scale Ferry model.

Load case number	Type of waves	Wave conditions	Mean foil submergence	Pitching shaft location (center of the wing) in ship fixed system
1	Head irregular waves	Hs = 0.07m f p= 0.67Hz	d=0.20-0.21m	x = 1.65 – 1.80m y = 0.0m, z =-0.085
2	Regular (harmonic) head waves	H = 0.06m f = 0.65Hz	d=0.20-0.21m	x = 1.65 – 1.80m y = 0.0m, z =-0.085
3	Regular (harmonic) head waves	H = 0.06m f = 0.75Hz	d=0.20-0.21m	x = 1.65 – 1.80m y = 0.0m, z =-0.085
4	Regular (harmonic) head waves	H = 0.06m f = 0.55Hz	d=0.20-0.21m	x = 1.65 – 1.80m y = 0.0m, z =-0.085

Table 3. Test cases of the UoS tank-scale bulk carrier model.

Parameter	Value
Wave Amplitude [m]	0.02
Wave Frequency [Hz]	0.65, 0.70, 0.75, 0.80, 0.85, 0.90, 0.95
Wavelength to ship length ratio (λ/L)	1.85, 1.59, 1.39, 1.22, 1.08, 0.96, 0.86
Ship Heading [degrees]	180 (head waves)
Ship Model Speed [m/s]	0.8
Froude Number ($V/\sqrt{gL}$)	0.18
SFC Force [N]	0.72 @ 15.5^{o}C

Measured data concerning the ship motion responses with and without the operation of the dynamic wing in head waves are presented in Fig.10(b), with and without the operation of the dynamic foil, for Froude number F=0.25, and the smaller draft of the ship. In the same figure the predictions obtained by the numerical models developed are also plotted using lines. It is observed that the operation of the foil leads to significant reduction of ship hull motion responses in a range of frequencies around the resonance, which is equivalent to reduction of added wave resistance and an overall increase of propulsion performance in waves.

In the case of UoS model at Froude number F=0.17 the measured results presented in Fig. 11 show an average reduction of approximately 10% and 20% in heave and pitch motions with the passive bow foil, respectively. The greatest reduction was observed at the wave frequency of 0.8Hz, which equates to a wavelength to ship length of approximately $\lambda / L = 1.2$. The UoS experiments show a significant reduction in delivered power in regular head waves, with the greatest reductions (up to 50%). The main effects of the foil system observed are twofold: (i) the foil generates a net thrust force, reducing the delivered power required to maintain a given speed in waves, and at the same time (ii) the foil reduces the pitch and heave motion of the vessel, reducing the added resistance in waves. Finally, indicative results from the experiments concerning the drop of added wave resistance and the enhancement of propulsion performance obtained from both models are presented in Fig.12.

4. Conclusions and future work directions

The results of the examined model scale tests show that the SeaTech dynamic wing technology provides a significant reduction in propulsive power required to maintain a constant speed of the ship in waves, offering also enhancement of stability due to the drop of responses. The free-running bulk carrier model demonstrated an average pitch and heave reduction of 20% and 10% respectively, and a reduction of delivered power of up to 50% for regular head waves near the resonance. Similar improvements of the order of 30% are reported in the case of the ferry ship model with an actively controlled flapping thruster, showing that the additional thrust generated by the dynamic wing will enable the engine to operate in part-load without compromising vessel speed, resulting in an additional positive effect on its emission profile, characterized by a significant reduction of NOx, SOx, CO_2 and particulate matter when the dynamic wing is combined with optimally controlled DF engine. The present results will support the design of full-size wing including strength, fatigue and service-life considerations, as well as actuation and mechanical wing-retractability system for calm and heavy weather conditions, respectively.

(a) (b)

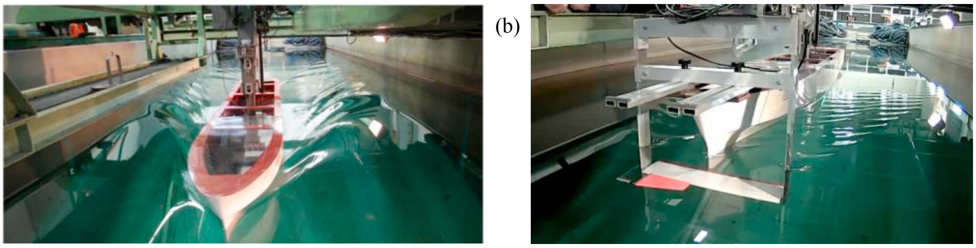

Fig. 8. Tank tests of the NTUA hull model in calm water: (a) without the dynamic wing, and (b) with the flapping thruster, and determination of calm-water resistance.

(a) (b)

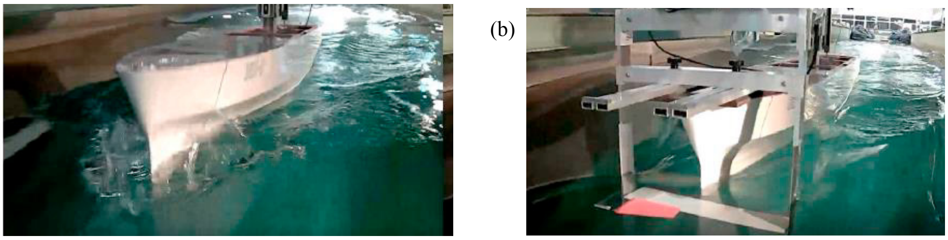

Fig. 9. Tank tests of the hull model in waves: (a) without the dynamic wing, and (b) with the flapping thruster, and determination of motions and total resistance.

(a) (b) (c)

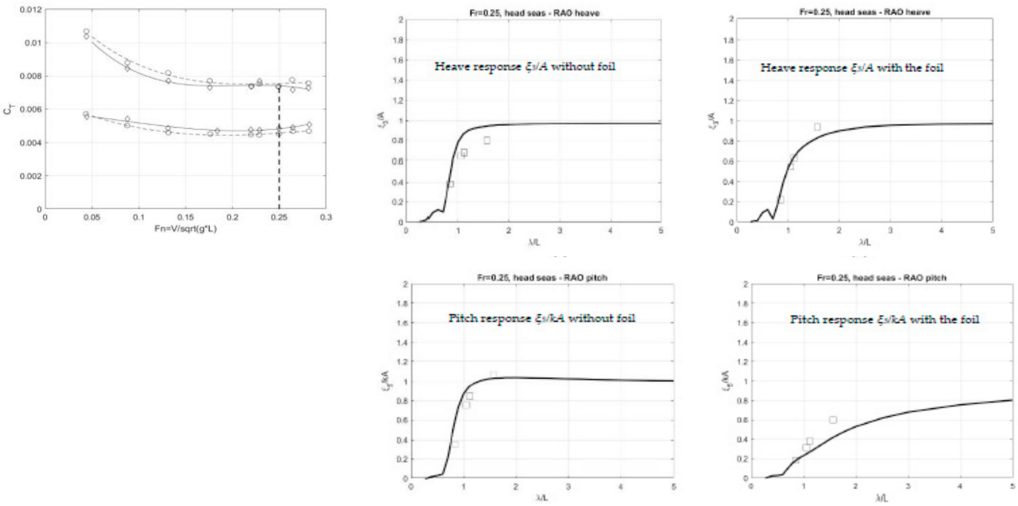

Fig. 10. Experimental data for the NTUA model. (a) Calm water resistance coefficient without and with the flapping thruster for various model speeds and corresponding Froude numbers, and the two drafts. Measured heave and pitch responses in head waves, (b) without and (c) with the operation of the dynamic foil, for Froude number F=0.25 and the smaller draft. Predictions by the developed numerical model, which is described in Belibassakis et al (2022), are shown using lines.

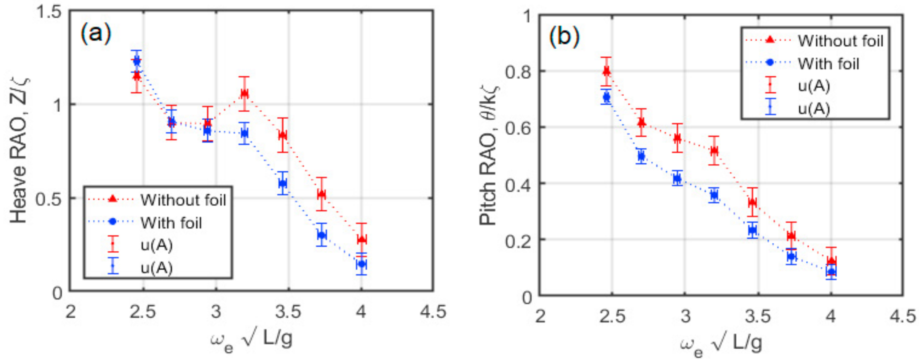

Fig. 11. Response Amplitude Operators (RAOs) for (a) heave, (b) pitch. Tto assess the repeatability (ITTC Type A uncertainty), 3 repeats at 2 frequencies were conducted and are included in the figures as error bars).

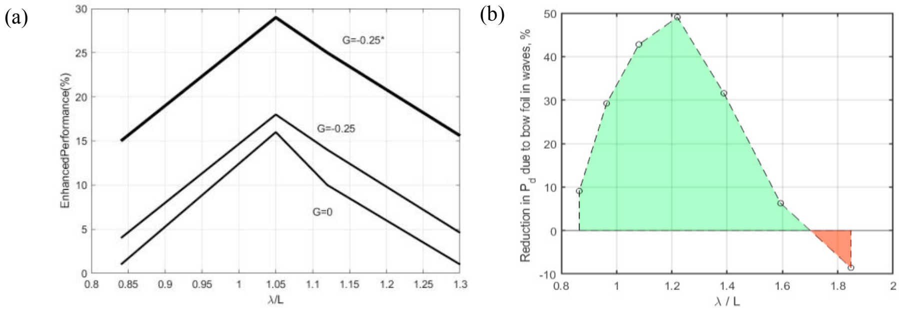

Fig. 12. Performance enhancement (a) due to dynamic foil operation at the bow of the NTUA tested Ferry ship model for various values of the gain G, and (b) due to the passive foil at the bow of the UoS Bulk Carrier model.

Acknowledgements

The present work has been supported by Seatech H2020 project received funding from the European Union's Horizon 2020 research and innovation program under the grant agreement No 857840. The opinions expressed in this document reflect only the author's view and in no way reflect the European Commission's opinions. The European Commission is not responsible for any use that may be made of the information it contains.

References

Belibassakis K.A., Politis G.K., 2013. Hydrodynamic performance of flapping wings for augmenting ship propulsion in waves, Ocean Engineering 72, 227-240.

Belibassakis K., Filippas E., Papadakis G., 2022. Numerical and Experimental Investigation of the Performance of Dynamic Wing for Augmenting Ship Propulsion in Head and Quartering Seas, J. Marine Science and Engineering 10, 24.

Filippas E., Papadakis, G., Belibassakis K.A., 2020. Free-Surface Effects on the Performance of Flapping-Foil Thruster for Augmenting Ship Propulsion in Waves, Journal Marine Science & Engineering, 8(5), 357.

Bøckmann E, Steen S., 2016. Model test and simulation of a ship with wavefoils. Applied Ocean Research 57, 8–18.

Bowker, J.A., Tan, M. and Townsend, N.C., 2020. Forward Speed Prediction of a Free-Running Wave-Propelled Boat. IEEE Journal of Oceanic Engineering, 46(2), 402-413.

Bowker J.A., Townsend N.C., 2022. Evaluation of bow foils on ship delivered power in waves using model tests, Appl. Ocean Research (to appear).

Rozhdestvensky K, Htet ZM, 2021. A Mathematical Model of a Ship with Wings Propelled by Waves. J. Marine Science Application 2021 1–26.

Triantafyllou M.S., Triantafyllou G.S., Yue D.K.P., 2000. Hydrodynamics of fishlike swimming. Annual Review of Fluid Mechanics 32, 33–53.

Wu X, Zhang X, Tian X, et al, 2020. A review on fluid dynamics of flapping foils. Ocean Engineering 195, 106712.